

# ChevOpt: Continuous-time State Estimation by Chebyshev Polynomial Optimization

Maoran Zhu, Yuanxin Wu

**Abstract**—In this paper, a new framework for continuous-time maximum a posteriori estimation based on the Chebyshev polynomial optimization (ChevOpt) is proposed, which transforms the nonlinear continuous-time state estimation into a problem of constant parameter optimization. Specifically, the time-varying system state is represented by a Chebyshev polynomial and the unknown Chebyshev coefficients are optimized by minimizing the weighted sum of the prior, dynamics and measurements. The proposed ChevOpt is an optimal continuous-time estimation in the least squares sense and needs a batch processing. A recursive sliding-window version is proposed as well to meet the requirement of real-time applications. Comparing with the well-known Gaussian filters, the ChevOpt better resolves the nonlinearities in both dynamics and measurements. Numerical results of demonstrative examples show that the proposed ChevOpt achieves remarkably improved accuracy over the extended/unscented Kalman filters and RTS smoother, close to the Cramer-Rao lower bound.

**Index Terms**— Nonlinear filter, Gaussian filter, Chebyshev polynomial, Collocation method, Maximum a posteriori estimation

## I. INTRODUCTION

The state estimation is to estimate the state of a system from the stochastic dynamic model and measurements. Thanks to many applications in spacecraft attitude determination [1, 2], robotics navigation [3, 4], biological process estimation [5], and many others, the state estimation algorithms have gained intensive research interests in the past decades.

The Bayesian framework, which computes the posterior density function of the state, provides an optimal solution to the state estimation [6]. For the linear and additive Gaussian noise system, the Kalman filter [7] is the optimal estimation method. However, for more general nonlinear systems with non-Gaussian noise, it is generally intractable to achieve the optimal estimation without any approximation.

Gaussian filters are a subset of Bayesian estimator for processing measurements up to the current time, under the assumption of Gaussian distribution for both states and noises [8-10]. A variety of Gaussian filters have been proposed in the literature to deal with the nonlinearity, which can be roughly classified into the Taylor expansion-based filter, the deterministic sampling-based filter and the Monte Carlo-based

filter [10, 11]. The most celebrated filter is the extended Kalman filter (EKF) [12], which approximates the nonlinearity of the state dynamics and measurement functions by successive first-order Taylor expansion at current estimate. EKF has been employed in vast practical applications, but it is prone to divergence due to the first order approximation. Second order Taylor expansion [13] is explored to decrease the approximation error, yet not commonly used in practice due to the cumbersome Hessian matrix. The iterated EKF is another strategy that tries to lessen the effect of the measurement nonlinearity by iteratively linearizing the measurement equation [13]. To further improve the state estimation accuracy, the backward smoother, which utilizes the measurements made before and after the current time, can be applied following the forward filter [14].

An alternative method to Gaussian filters for addressing nonlinearity is to utilize a set of deterministic sampling points to approximate the probability distribution. The unscented Kalman filter (UKF) [15, 16] generates the sigma points, according to the known prior density, and utilizes the unscented transformation to propagate statistical information of the posteriori density. The quadrature Kalman filter is proposed in [9, 10, 17] for both discrete and continuous systems from the standpoint of Gauss-Hermite numerical quadrature. The works [18, 19] utilize the cubature rule to numerically approximate integrals and build the cubature Kalman filter. The advantage of these sampling-based filters is that they avoid evaluating the cumbersome Jacobian/Hessian matrix and do not require dynamics and measurement functions to be smooth and differentiable. In contrast to the deterministic sampling filter, the Monte Carlo-based particle filter [20-22] draws a large number of random samples to approximate and propagate the probability distribution, which promises to be the best state estimation algorithm. However, the exponential increase of samples with the dimensionality of the state space leads to a great computation burden.

Another class of methods related to this paper is the optimization-based state estimation. The works [23, 24] propose an efficient incremental optimization algorithm based on the factor graph to decrease the computation burden in optimization-based batch estimation. And, [25-27] propose the so-called moving horizon estimation (MHE), which optimizes the discrete-time state in a sliding window with the objective function being formed by the dynamics, measurements and

This paper was supported in part by National Key R&D Program of China (2018YFB1305103).

Author's address: M. Zhu and Y. Wu are with Shanghai Key Laboratory of Navigation and Location-based Services, School of Electronic Information and

Electrical Engineering, Shanghai Jiao Tong University, Shanghai 200240, China (email: zhumaoran@sjtu.edu.cn, yuanx\_wu@hotmail.com).

assumed prior distribution. As for the continuous-time estimation, the works [28-30] initiate a batch maximum a posteriori (MAP) estimation method based on the B-spline function approximation for the simultaneous localization and mapping problem. However, the state estimate by the low-order B-spline is not accurate enough and the approximation error has to be remedied through the weighting matrix [31, 32]. Besides, the batch estimation cannot be applied to the real-time applications.

In this paper, we try to introduce the Chebyshev collocation method to solve the continuous-time state estimation problem. The collocation method is a well-known numerical algorithm for solving differential equations, which is to find a polynomial that satisfies the differential equations at a number of given points, namely, the collocation points [33, 34]. Owing to its efficiency and high accuracy, the collocation method has received many applications, including but not limited to fluid dynamics [35, 36], optimal control [37-39] and orbit propagation problems [40, 41]. The work [42] proposes a Chebyshev collocation-based batch state and dynamics estimation. However, it is more like trajectory optimization [39] than the general state estimation with priori information, covariance propagation and probabilistic interpretation [43]. Besides, the dynamics constraints at the discrete Chebyshev points therein are not optimal in the MAP sense and the batch method is not friendly to real-time applications.

The current paper is an extension from a series of works [44-47], in which the Chebyshev polynomial has been used to fully represent the rigid motion including attitude, velocity and position, and to numerically solve the involved motion dynamics, namely the forward propagation counterpart in state estimation. The motivation of this paper is to extend the Chebyshev's representation to incorporate the measurements and consequently to better solve the state estimation problem. Specifically, the continuous-time state in the time interval of interest is to be represented by a Chebyshev polynomial, and the continuous MAP state estimation is then transformed into a problem of Chebyshev coefficients optimization through the Chebyshev collocation method, named as the ChevOpt in this paper. Comparing with other kinds of polynomials, the Chebyshev polynomial is more accurate and very close to the best polynomial in the  $\infty$ -norm [34]. To meet the requirement of real-time applications, we further come up with a recursive sliding-window version (named as ChevFilter), inspired by the strategy in MHE. It is noted that the model and noise are assumed well known and the influence of the model error and uncertainty [48, 49] is not considered in the current paper, although they should be seriously treated in any practical system.

The main contribution of this work rests on a novel framework of continuous-time state estimation based on the Chebyshev polynomial in both batch and sliding-window forms. Comparing with well-known Gaussian filters, the proposed estimation does not introduce any approximation of the nonlinear dynamics and measurements and thus achieves remarkably improved accuracy. The remaining of the paper is organized as follows. Section II reviews the continuous-time

batch MAP estimation problem. After a brief introduction of the Chebyshev collocation method, Section III proposes the optimal state estimation framework - ChevOpt. To meet the requirement of real-time applications, the ChevFilter is proposed in Section IV, which reformulates the batch ChevOpt algorithm in a sliding window with a covariance propagation algorithm. Section V is devoted to assessing the proposed algorithms and demonstrating their accuracy against traditional Gaussian filters. The discussions and conclusions are finally drawn in Section VI.

## II. BATCH MAP ESTIMATION

The commonly-employed strategy of state estimation is maximum a posteriori, which is to find the most likely posterior state given the knowledge of prior, measurements and the dynamics model [13]. This section will review the probabilistic formulation of the batch MAP estimation for the nonlinear continuous-discrete system.

Consider a continuous-discrete nonlinear system, defined on the time interval  $t \in [t_0, t_M]$  in the form of dynamic state-space model, as

$$\begin{aligned}\dot{\mathbf{x}}(t) &= \mathbf{f}(\mathbf{x}(t), \mathbf{u}(t)) + \mathbf{G}(t)\mathbf{w}(t) \\ \mathbf{z}_k &= \mathbf{h}(\mathbf{x}_k) + \mathbf{v}_k\end{aligned}\quad (1)$$

where  $\mathbf{x}(t) \in \mathbb{R}^n$  denotes the time-varying state,  $\mathbf{z}_k \in \mathbb{R}^m$  denotes the measurement at time  $t_k$ .  $\mathbf{f}(\cdot): \mathbb{R}^n \rightarrow \mathbb{R}^n$  and  $\mathbf{h}(\cdot): \mathbb{R}^n \rightarrow \mathbb{R}^m$  are known continuous and smooth functions.  $\mathbf{G}(t) \in \mathbb{R}^{n \times m}$  is the noise driven matrix,  $\mathbf{u}(t) \in \mathbb{R}^p$  is the deterministic known control input, and  $\mathbf{w}(t) \in \mathbb{R}^m$  is the zero-mean Gaussian dynamics noise with the covariance given by

$$E\{\mathbf{w}(t)\mathbf{w}^T(\tau)\} = \mathbf{Q}\delta(t-\tau) \quad (2)$$

where  $\delta(\cdot)$  is the Dirac's delta function.  $\mathbf{v}_k \sim N(\mathbf{0}, \mathbf{R}_k)$  is the measurement Gaussian noise, which is uncorrelated with  $\mathbf{w}(t)$ . Suppose that the priori state estimate  $\mathbf{x}(t_0)$  is Gaussian-distributed, i.e.,  $\mathbf{x}(t_0) \sim N(\hat{\mathbf{x}}_0, \mathbf{P}_0)$ . The goal of the MAP estimation is to find the best estimate for the state of the system  $\mathbf{x}(t)$ , given the prior information  $\hat{\mathbf{x}}_0$ , control input  $\mathbf{u}$  and a sequence of measurements  $\mathbf{z}_{1:M} \triangleq \{\mathbf{z}_1 \cdots \mathbf{z}_M\}$

$$\hat{\mathbf{x}}(t) = \arg \max_{\mathbf{x}} p(\mathbf{x} | \mathbf{u}, \mathbf{z}_{1:M}) \quad (3)$$

where  $p(\mathbf{x} | \mathbf{u}, \mathbf{z}_{1:M})$  is the posterior probability density function (PDF) over the state. Using the Bayesian rule, (3) is equivalent to

$$\begin{aligned}\hat{\mathbf{x}}(t) &= \arg \max_{\mathbf{x}} \frac{p(\mathbf{z}_{1:M} | \mathbf{x}, \mathbf{u}) p(\mathbf{x} | \mathbf{u})}{p(\mathbf{z}_{1:M} | \mathbf{u})} \\ &\sim \arg \max_{\mathbf{x}} p(\mathbf{z}_{1:M} | \mathbf{x}, \mathbf{u}) p(\mathbf{x} | \mathbf{u})\end{aligned}\quad (4)$$

where  $p(\mathbf{z}_{1:M} | \mathbf{x}, \mathbf{u})$  is the likelihood function of measurements and  $p(\mathbf{x} | \mathbf{u})$  denotes the evolution of the state.

The denominator in (4) is dropped because it does not depend on  $\mathbf{x}$  [3, 13].

Define the weighted residuals of initial state, measurements and dynamics, respectively, as

$$\begin{aligned}\mathbf{e}_{\mathbf{x}_0} &= \mathbf{W}_{\mathbf{x}_0}^T (\mathbf{x}(t_0) - \hat{\mathbf{x}}_0) \\ \mathbf{e}_{\mathbf{z}_k} &= \mathbf{W}_{\mathbf{z}_k}^T (\mathbf{z}_k - \mathbf{h}(\mathbf{x}_k)) \\ \mathbf{e}_v(t) &= \mathbf{W}_v^T (\dot{\mathbf{x}}(t) - \mathbf{f}(\mathbf{x}(t), \mathbf{u}(t)))\end{aligned}\quad (5)$$

where  $\mathbf{W}_{\mathbf{x}_0}$ ,  $\mathbf{W}_{\mathbf{z}_k}$  and  $\mathbf{W}_v$  are lower triangular matrixes, obtained by the Cholesky factorization of  $\mathbf{P}_0^{-1}$ ,  $\mathbf{R}_k^{-1}$  and  $(\mathbf{GQG})^{-1}$ , that is to say,  $\mathbf{P}_0^{-1} = \mathbf{W}_{\mathbf{x}_0} \mathbf{W}_{\mathbf{x}_0}^T$ ,  $\mathbf{R}_k^{-1} = \mathbf{W}_{\mathbf{z}_k} \mathbf{W}_{\mathbf{z}_k}^T$  and  $(\mathbf{GQG})^{-1} = \mathbf{W}_v \mathbf{W}_v^T$ .

Because the noises  $\mathbf{v}_k$  and  $\mathbf{w}(t)$  are uncorrelated, the likelihood function of the measurements can be simplified as

$$p(\mathbf{z}_{1:M} | \mathbf{x}, \mathbf{u}) = \eta_1 \prod_{k=1}^M \exp \left\{ -\frac{1}{2} \mathbf{e}_{\mathbf{z}_k}^T \mathbf{e}_{\mathbf{z}_k} \right\} \quad (6)$$

where  $\eta_1$  is the normalization constant factor. And the probability density of  $p(\mathbf{x} | \mathbf{u})$  in (4) is written as [43]

$$p(\mathbf{x} | \mathbf{u}) = \eta_2 p(\mathbf{x}_0) \exp \left\{ -\frac{1}{2} \int_{t_0}^{t_M} \mathbf{e}_v(t)^T \mathbf{e}_v(t) dt \right\} \quad (7)$$

where  $\eta_2$  is the normalization constant factor. Substituting (6) and (7) into (4) and taking the negative logarithm of the probability density functions, the MAP estimation is transformed to the following optimization problem

$$\hat{\mathbf{x}}(t) = \arg \min_{\mathbf{x}} \left( J_{\mathbf{x}_0} + J_{\mathbf{z}_{1:M}} + J_{\mathbf{v}_{[t_0, t_M]}} \right) \quad (8)$$

where  $J_{\mathbf{x}_0}$ ,  $J_{\mathbf{z}_{1:M}}$  and  $J_{\mathbf{v}_{[t_0, t_M]}}$  are defined as

$$\begin{aligned}J_{\mathbf{x}_0} &= \mathbf{e}_{\mathbf{x}_0}^T \mathbf{e}_{\mathbf{x}_0} \\ J_{\mathbf{z}_{1:M}} &= \sum_{k=1}^M \mathbf{e}_{\mathbf{z}_k}^T \mathbf{e}_{\mathbf{z}_k} \\ J_{\mathbf{v}_{[t_0, t_M]}} &= \int_{t_0}^{t_M} \mathbf{e}_v(t)^T \mathbf{e}_v(t) dt\end{aligned}\quad (9)$$

The estimation problem in (8) is an infinite-dimension functional optimization, which can be transformed into a finite parameter optimization problem by the Chebyshev collocation method to be discussed in the sequel.

It is noted that in the computation of weighted matrices in (5), the dynamics-related term  $\mathbf{GQG}^T$  is assumed to be positive definite, which may not be satisfied in many applications. This issue can be handled by dividing the dynamics into the sub-dynamics with a positive definite noise matrix and a noise-free sub-dynamics [47] (See details in the Appendix). Furthermore, there are several strategies to handle the issue to be discussed in detail in Section IV.

### III. BATCH MAP ESTIMATION VIA CHEBYSHEV POLYNOMIAL

#### A. Chebyshev Polynomial and Collocation Method

The Chebyshev polynomial basis is defined over the interval  $[-1, 1]$  by the recurrence relation as

$$\begin{aligned}F_0(\tau) &= 1, F_1(\tau) = \tau, \\ F_{i+1}(\tau) &= 2\tau F_i(\tau) - F_{i-1}(\tau) \quad \text{for } i \geq 1\end{aligned}\quad (10)$$

where  $F_i(\tau)$  is the  $i^{\text{th}}$ -degree Chebyshev polynomial of the first kind. The derivative of the Chebyshev polynomial is obtained by differentiating (10), as

$$\begin{aligned}\dot{F}_0(\tau) &= 0, \dot{F}_1(\tau) = 1, \\ \dot{F}_{i+1}(\tau) &= 2F_i(\tau) + 2\tau \dot{F}_i(\tau) - \dot{F}_{i-1}(\tau) \quad \text{for } i \geq 1\end{aligned}\quad (11)$$

where  $\dot{F}_i(\tau)$  denotes the derivative of the  $i^{\text{th}}$ -degree Chebyshev polynomial. And the integrated  $i^{\text{th}}$ -degree Chebyshev polynomial can be expressed as a linear combination of  $(i+1)^{\text{th}}$ -degree Chebyshev polynomial, given by [50]

$$G_{i,[-1,\tau]} = \int_{-1}^{\tau} F_i(\tau) d\tau = \begin{cases} \left( \frac{F_{i+1}(\tau)}{2(i+1)} - \frac{F_{i-1}(\tau)}{2(i-1)} \right) - \frac{(-1)^i}{i^2-1} F_0(\tau), & i \neq 1 \\ \frac{F_{i+1}(\tau)}{4} - \frac{F_0(\tau)}{4}, & i = 1 \end{cases} \quad (12)$$

Consider a nonlinear differential equation on  $t \in [a, b]$

$$f(\dot{y}(t), y(t), t) = 0 \quad (13)$$

where  $f(\cdot)$  is a smooth function and  $y$  is the solution of interest. In order to use the Chebyshev polynomial, the original interval is mapped into  $\tau \in [-1, 1]$  by the affine transformation

$$\tau = \frac{2}{b-a} t - \frac{b+a}{b-a} \quad (14)$$

Then, the function  $y$  can be approximated by the Chebyshev polynomial of degree  $N$ , together with its derivative  $\dot{y}$ , as

$$y(\tau) \approx y_N(\tau) = \sum_{i=0}^N c_i F_i(\tau) \quad (15)$$

$$\dot{y}(\tau) \approx \dot{y}_N(\tau) = \sum_{i=0}^N c_i \dot{F}_i(\tau) \quad (16)$$

where  $c_i$  is the Chebyshev coefficient to be determined. The collocation method [33] approximates the solution  $y(\tau)$  by the polynomial  $y_N(\tau)$  of degree  $N$ , which satisfies the differential equation at the chosen collocation points  $\tau_k \in [-1, 1]$  for  $k=0, \dots, N$ , as follows

$$f(\dot{y}(\tau_k), y(\tau_k), \tau_k) = 0 \quad k=0, 1, \dots, N \quad (17)$$

Generally, the collocation points associated with Chebyshev polynomial are taken as the Chebyshev points, i.e.,

$$\tau_k = -\cos(k\pi/N), \quad k=0, 1, \dots, N \quad (18)$$

Substituting (15), (16) and (18) into (17), the nonlinear differential equation is transformed into nonlinear equations about the Chebyshev coefficient  $c_k$ , which can be solved by many optimization algorithms, e.g., the Newton method [33].

Interested readers are referred to [33, 51] and references therein for more details about the collocation method.

Instead of estimating the Chebyshev coefficients in (16), the objective function can also be constructed using the unknown states at the collocation points [52]. In fact, the function  $u$  can be equally represented by its value at each collocation point or the Chebyshev coefficients, and the transformation of these two representations can be realized efficiently by the Fast Fourier Transform [34].

### B. Batch MAP Estimation Via Collocation Method

The objective function for the batch MAP estimation in (8) can be solved by the Chebyshev collocation method. Transforming the time interval  $[t_0 \ t_M]$  to  $[-1 \ 1]$  by (14) and approximating the state and its derivative by Chebyshev polynomials as

$$\mathbf{x}(\tau) \approx \mathbf{x}_N(\tau) \triangleq \sum_{i=0}^N \mathbf{d}_i F_i(\tau) \quad (19)$$

$$\dot{\mathbf{x}}(\tau) \approx \dot{\mathbf{x}}_N(\tau) = \sum_{i=0}^N \mathbf{d}_i \dot{F}_i(\tau) \quad (20)$$

where  $\mathbf{d}_i \in \mathbb{R}^n$  is the  $i^{\text{th}}$ -degree Chebyshev coefficient to be determined. With these approximations, the batch MAP estimation in (8) is transformed into the parameter optimization problem as

$$\mathbf{d}_{0:N} = \arg \min_{\mathbf{d}_{0:N}} \left( J'_{\mathbf{x}_0} + J'_{\mathbf{z}_{1:M}} + J'_{\mathbf{v}_{[-1,1]}} \right) \quad (21)$$

where  $\mathbf{d}_{0:N} \triangleq [\mathbf{d}_0^T, \dots, \mathbf{d}_N^T]^T$  and the terms  $J'_{\mathbf{x}_0}$ ,  $J'_{\mathbf{z}_{1:M}}$  and  $J'_{\mathbf{v}_{[-1,1]}}$  are defined as

$$\begin{aligned} J'_{\mathbf{x}_0} &= \mathbf{e}'_{\mathbf{x}_0}^T \mathbf{e}'_{\mathbf{x}_0} \\ J'_{\mathbf{z}_{1:M}} &= \sum_{k=1}^M \mathbf{e}'_{\mathbf{z}_k}^T \mathbf{e}'_{\mathbf{z}_k} \\ J'_{\mathbf{v}_{[-1,1]}} &= \frac{t_M - t_0}{2} \int_{-1}^1 \mathbf{e}'_{\mathbf{v}}(\tau)^T \mathbf{e}'_{\mathbf{v}}(\tau) d\tau \end{aligned} \quad (22)$$

where  $\mathbf{e}'_{\mathbf{x}_0}$ ,  $\mathbf{e}'_{\mathbf{z}_k}$  and  $\mathbf{e}'_{\mathbf{v}}$  are the weighted residuals of initial state, measurements and dynamics, respectively, in the form of Chebyshev polynomials

$$\begin{aligned} \mathbf{e}'_{\mathbf{x}_0} &= \mathbf{W}_{\mathbf{x}_0}^T (\mathbf{x}_N(-1) - \hat{\mathbf{x}}_0) \\ \mathbf{e}'_{\mathbf{z}_k} &= \mathbf{W}_{\mathbf{z}_k}^T (\mathbf{z}_k - \mathbf{h}(\mathbf{x}_N(\tau_k))) \\ \mathbf{e}'_{\mathbf{v}}(\tau) &= \mathbf{W}_{\mathbf{v}}^T \left( \frac{2}{t_M - t_0} \dot{\mathbf{x}}_N(\tau) - \mathbf{f}(\mathbf{x}_N(\tau), \mathbf{u}(\tau)) \right) \end{aligned} \quad (23)$$

The integrated term  $J'_{\mathbf{v}_{[-1,1]}}$  in (21) can be approximated by the Clenshaw-Curtis quadrature [34] formula as

$$J'_{\mathbf{v}_{[-1,1]}} \approx \frac{t_M - t_0}{2} \sum_{i=0}^N \omega_i \mathbf{e}'_{\mathbf{v}}(\tau_i)^T \mathbf{e}'_{\mathbf{v}}(\tau_i) \quad (24)$$

where  $\omega_i$  is the weight to be predetermined by the integral of the Lagrange polynomial

$$\omega_i = \int_{-1}^1 \ell_i(\tau) d\tau \quad (25)$$

and the Lagrange polynomial is given as

$$\ell_i(\tau) = \prod_{k=0, k \neq i}^N (\tau - \tau_k) / \prod_{k=0, k \neq i}^N (\tau_k - \tau_i) \quad (26)$$

Substituting (24) into (21), the optimization problem is transformed into a nonlinear least squares problem about  $\mathbf{d}_{0:N}$ , which can be solved by a number of algorithms, e.g. the Levenberg-Marquardt method [53]. With the optimized parameter  $\mathbf{d}_{0:N}$ , the state over the whole time interval is then acquired by (19).

The state approximation by the Chebyshev polynomial in (19) and the Clenshaw-Curtis quadrature in (24) are the only two approximations in the proposed ChevOpt framework. As for state approximation, the Chebyshev polynomial is very close to the best polynomial approximation in the  $\infty$ -norm [34]. On the other hand, the Clenshaw-Curtis quadrature converges for any continuous function [54]. With the increased order of Chebyshev polynomial  $N$ , these approximation errors will approach zero. It means that the proposed ChevOpt is optimal in the least squares sense insofar as the number of collocation points are sufficiently large.

### IV. CHEVFILTER: RECURSIVE MAP ESTIMATION VIA CHEBYSHEV POLYNOMIAL

Since the batch ChevOpt can only be implemented until all the measurements come in, we turn to solve the MAP estimation by ChevOpt in a sliding time window, named as ChevFilter hereafter.

Assume the current sliding window is  $[t_{m-I} \ t_m]$ , where  $I$  is the size of the sliding window. Following (21)-(23), the MAP estimation in the sliding window can be readily formulated as

$$\mathbf{d}_{0:N} = \arg \min_{\mathbf{d}_{0:N}} \left( J'_{\mathbf{x}_{m-I}} + J'_{\mathbf{z}_{m-I+1:M}} + J'_{\mathbf{v}_{[-1,1]}} \right) \quad (27)$$

where  $J'_{\mathbf{x}_{m-I}}$  is the state prior including and before  $t_{m-I}$ , and the terms are defined as follows

$$\begin{aligned} J'_{\mathbf{x}_{m-I}} &= \mathbf{e}'_{\mathbf{x}_{m-I}}^T \mathbf{e}'_{\mathbf{x}_{m-I}} \\ J'_{\mathbf{z}_{m-I+1:M}} &= \sum_{k=m-I+1}^m \mathbf{e}'_{\mathbf{z}_k}^T \mathbf{e}'_{\mathbf{z}_k} \\ J'_{\mathbf{v}_{[-1,1]}} &= \frac{t_m - t_{m-I}}{2} \int_{-1}^1 \mathbf{e}'_{\mathbf{v}}(\tau)^T \mathbf{e}'_{\mathbf{v}}(\tau) d\tau \end{aligned} \quad (28)$$

where

$$\begin{aligned} \mathbf{e}'_{\mathbf{x}_{m-I}} &= \mathbf{W}_{\mathbf{x}_{m-I}}^T (\mathbf{x}_N(-1) - \hat{\mathbf{x}}_{m-I}) \\ \mathbf{e}'_{\mathbf{z}_k} &= \mathbf{W}_{\mathbf{z}_k}^T (\mathbf{z}_k - \mathbf{h}(\mathbf{x}_N(\tau_k))) \\ \mathbf{e}'_{\mathbf{v}}(\tau) &= \mathbf{W}_{\mathbf{v}}^T \left( \frac{2}{t_m - t_{m-I}} \dot{\mathbf{x}}_N(\tau) - \mathbf{f}(\mathbf{x}_N(\tau), \mathbf{u}(\tau)) \right) \end{aligned} \quad (29)$$

The weight matrix  $\mathbf{W}_{\mathbf{x}_{m-I}}$  is obtained by the Cholesky factorization of  $\mathbf{P}_{m-I}^{-1}$  as  $\mathbf{P}_{m-I}^{-1} = \mathbf{W}_{\mathbf{x}_{m-I}} \mathbf{W}_{\mathbf{x}_{m-I}}^T$ .

To acquire the initial covariance  $\mathbf{P}_{m-I}$  at the beginning of a sliding window, a convenient strategy is to approximate the prior as a Gaussian distribution and use the extended Kalman filter for covariance prediction and update [26] with the state

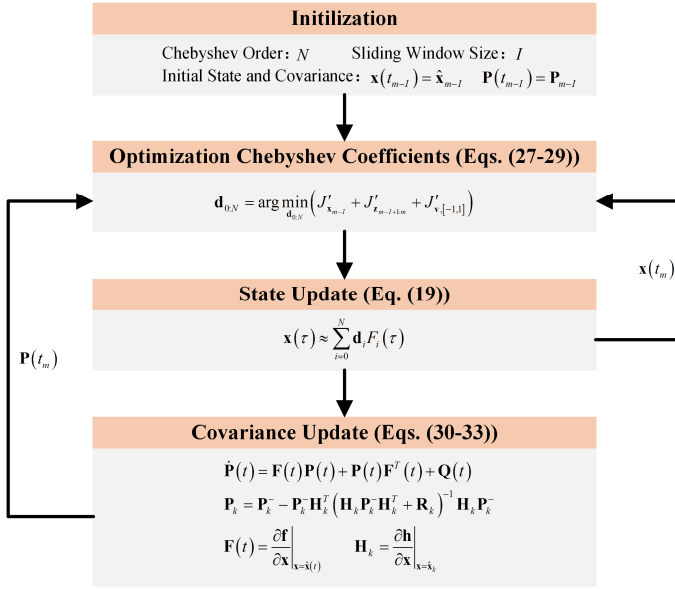


Fig. 1. Flowchart of the ChevFilter

estimated by ChevFilter. Specifically, for a continuous-discrete system, the EKF prediction covariance is governed by [13]

$$\dot{\mathbf{P}}(t) = \mathbf{F}(t)\mathbf{P}(t) + \mathbf{P}(t)\mathbf{F}^T(t) + \mathbf{Q}(t) \quad (30)$$

where  $\mathbf{F}(\bullet)$  is the Jacobian function of dynamics. Instead of using the prediction state by EKF,  $\mathbf{F}(\bullet)$  is evaluated at the estimated state by ChevFilter

$$\mathbf{F}(t) = \left. \frac{\partial \mathbf{f}}{\partial \mathbf{x}} \right|_{\mathbf{x}=\hat{\mathbf{x}}(t)} \quad (31)$$

The integral of (30) can be solved by either the traditional Runge-Kutta or the Chebyshev collocation method as well. When it comes to the measurement at time  $t_k$ , the predicted covariance is updated by

$$\mathbf{P}_k = \mathbf{P}_k^- - \mathbf{P}_k^- \mathbf{H}_k^T (\mathbf{H}_k \mathbf{P}_k^- \mathbf{H}_k^T + \mathbf{R}_k)^{-1} \mathbf{H}_k \mathbf{P}_k^- \quad (32)$$

where  $\mathbf{P}_k^-$  is the predicted covariance at time  $t_k$  by (30), and  $\mathbf{H}_k$  is the Jacobian of  $\mathbf{h}(\cdot)$  also evaluated at the estimated state in the sliding window by ChevFilter

$$\mathbf{H}_k = \left. \frac{\partial \mathbf{h}}{\partial \mathbf{x}} \right|_{\mathbf{x}=\hat{\mathbf{x}}_k} \quad (33)$$

Figure 1 lists the main steps of the ChevFilter. The estimation is initialized with the user-given Chebyshev order, sliding window size, initial state and corresponding covariance. The Chebyshev coefficients of the state are estimated by minimizing the objective function in (27) and the initial coefficients of the optimization can be acquired by ChevFilter with a smaller window size or the fitting polynomial of the EKF result. After the optimization, the continuous state over the sliding window is obtained by the Chebyshev polynomial approximation. And, the corresponding covariance is calculated by EKF with the linearized dynamics and measurement at the ChevFilter estimated state. Finally, the estimated state and covariance at the end of the sliding window are treated as the prior for the next sliding window.

In the case of semi-positive definite  $\mathbf{G}\mathbf{Q}\mathbf{G}^T$  as discussed in Section II and Appendix, the dynamics can be divided into the sub-dynamics with a positive definite noise matrix and the noise-free sub-dynamics. The proposed ChevOpt framework can be used on the positive definite sub-dynamics directly. And, for the noise-free sub-dynamics, there are several strategies to handle it as follows:

- If the noise-free sub-dynamics function  $\mathbf{g}^{(2)}(\mathbf{y}(t), \mathbf{u}(t))$  in (51) does not depend on the noise-free state  $\mathbf{y}^{(2)}$  at all, i.e.,  $\mathbf{g}^{(2)}(\mathbf{y}(t), \mathbf{u}(t)) \equiv \mathbf{g}^{(2)}(\mathbf{y}^{(1)}(t), \mathbf{u}(t))$ ,  $\mathbf{y}^{(2)}$  can be removed from the estimation and represented as a function of the remaining state  $\mathbf{y}^{(1)}$ . (See Examples 1-2 in Section V)
- Remove the noise-free part of the dynamics from the objective function and treat it instead as a constraint in the optimization (21) or (27).
- Add a small disturbance to the noise-free sub-dynamics to make the noise covariance positive definite (See Example 2 about the velocity  $x_2$ ). This strategy has been commonly used in the traditional state estimation methods, see e.g., [16] and [55].

Note that the first strategy helps decrease the state space dimensionality, which is preferable than the other two strategies in reducing computation burden. The third strategy is approximate in terms of adding pseudo-noises, while the second strategy is most time-consuming due to the constrained optimization.

## V. SIMULATIONS AND RESULTS

In this section, we will evaluate the proposed batch ChevOpt and recursive ChevFilter by two representative estimation examples, viz. the Van der Pol model and the ballistic target reentry, which have been extensively investigated in the literature [9, 14, 15, 56], and compare with EKF, UKF and the batch Rauch, Tung, and Striebel (RTS) smoother. All the mentioned algorithms in this paper are performed on the MATLAB platform and the function 'lsqnonlin' with analytical Jacobian is used to solve the nonlinear optimization in both ChevOpt and ChevFilter. Besides, the Cramer-Rao lower bound (CRLB) [11, 57] is presented as the reference of performance comparison, as it sets a theoretical limit on the best achievable performance of any filter, which admits us to quantify how much scope is left to improve a filter [8]. Specifically, the covariance of the any estimate is bounded by

$$\mathbf{E}[(\hat{\mathbf{x}} - \mathbf{x})(\hat{\mathbf{x}} - \mathbf{x})^T] \geq \mathbf{CRLB} \quad (34)$$

And, the CRLB is equal to the inverse of the information matrix  $\mathbf{J}$ , which is calculated recursively [57] as

$$\mathbf{J}_{k+1} = \mathbf{E}[\mathbf{H}_{k+1}^T \mathbf{R}_{k+1}^{-1} \mathbf{H}_{k+1}] + \mathbf{Q}_k^{-1} - \mathbf{Q}_k^{-1} \mathbf{E}(\mathbf{F}_k) (\mathbf{J}_k + \mathbf{E}[\mathbf{F}_k^T \mathbf{Q}_k^{-1} \mathbf{F}_k])^{-1} \mathbf{E}(\mathbf{F}_k^T) \mathbf{Q}_k^{-1} \quad (35)$$

where  $\mathbf{E}(\cdot)$  denotes the computation of expectation.  $\mathbf{F}_k$  and  $\mathbf{H}_{k+1}$  are the Jacobians of the dynamic and measurement

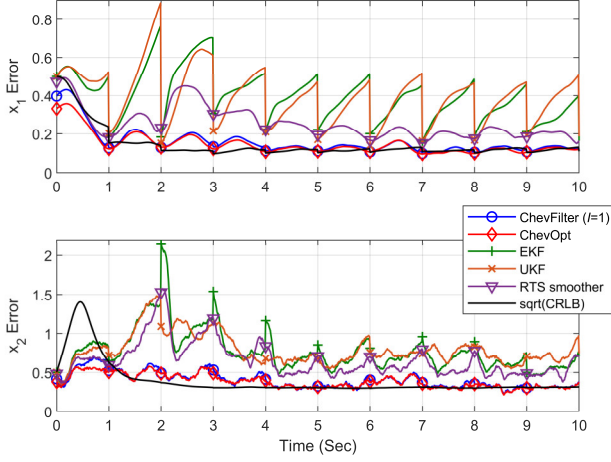


Fig. 2. Averaged absolute errors of the state (ChevFilter with window size of 1s) and the square root of CRLB.

models, evaluated at the true state at time  $t_k$  and  $t_{k+1}$ , respectively.

#### A. Example 1: Van der Pol Oscillator

The Van der Pol's equation is defined in the state-space model as [56]

$$\begin{aligned}\dot{x}_1 &= x_2 + w_1 \\ \dot{x}_2 &= -\lambda(x_1^2 - 1)x_2 - x_1 + w_2\end{aligned}\quad (36)$$

where  $[w_1 \ w_2]^T \sim N(\mathbf{0}, \mathbf{Q}_c)$  is the continuous dynamics noise and  $\mathbf{x} \triangleq [x_1 \ x_2]^T$  is the state vector. The parameter  $\lambda$  is a constant value ( $\lambda = 3$ ). The measurement equation at time  $t_k$  is given as

$$z_k = x_1(t_k) + v_k \quad (37)$$

where  $v_k \sim N(0, R_k)$  is the white measurement noise and the frequency of the measurement is assumed to be 1 Hz.

The spectral density of the continuous dynamics noise is  $\mathbf{Q}_c = \begin{bmatrix} 0 & 0 \\ 0 & 1 \end{bmatrix}$  and the measurement noise covariance is  $R_k = 0.04$ . The reference in the simulation is generated over a time period of 10 seconds using the Euler-Maruyama method [58] at the time step  $\Delta t = 5 \times 10^{-4}$  s, with the true initial state  $\mathbf{x}_0 = [0.5 \ 0.5]^T$ . The relationship between the spectral density and the discrete covariance is approximated as  $\mathbf{Q}_d \approx \mathbf{Q}_c \Delta t$ .

For all estimators, the initial state is  $\hat{\mathbf{x}}_0 = [1 \ 1]^T$  with the covariance

$$P_0 = \begin{bmatrix} 0.25 & 0 \\ 0 & 0.25 \end{bmatrix}$$

The step size of prediction for EKF, UKF and RTS smoother is 0.01s.

In this example, the first strategy listed in Section IV is applied to handle the semi-positive dynamics noise covariance,

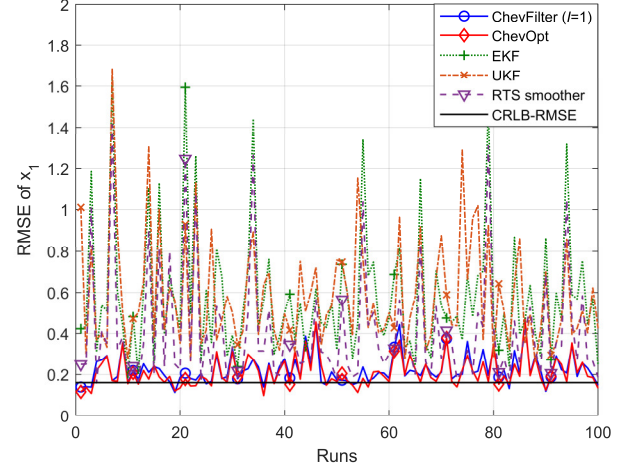


Fig. 3. RMSE of  $x_1$  (ChevFilter with window size of 1s) across 100 random runs and CRLB-RMSE.

where the state component  $x_2$  is approximated by the Chebyshev polynomial and  $x_1$  is obtained by the integral of  $x_2$

$$\begin{aligned}x_1(\tau) &\approx p_0 + \sum_{i=0}^N c_i G_{i,[-1,\tau]} \\ x_2(\tau) &\approx \sum_{i=0}^N c_i F_i(\tau)\end{aligned}\quad (38)$$

where  $c_i$  is the Chebyshev coefficient to be determined,  $p_0$  is the initial value of  $x_1$  at the left end of sliding window, and  $G_{i,[-1,\tau]}$  is the integral of Chebyshev polynomial  $F_i(\tau)$  as given in (12). By so doing, the semi-positive definite dynamics noise covariance is naturally circumvented and the state dimensionality of the nonlinear optimization is also reduced by a half.

The estimation parameters in this example  $\mathbf{d} \triangleq [p_0 \ c_{0,N}^T]$  include the Chebyshev coefficients and initial position, which are determined by substituting (38) into (21) for ChevOpt or (27) for ChevFilter, respectively. The time window size of ChevFilter is set to 1 second. The Chebyshev polynomial orders  $N$  are set to 300 and 20 for ChevOpt and ChevFilter, respectively.

As per (36), the CRLB computation requires an invertible dynamics noise covariance. A small value is assumed for  $w_1$ , namely,  $w_1 \sim N(0, 0.001^2)$ , to make the dynamics noise covariance invertible. The averaged absolute error of  $i$ -th state component at time  $k$  is defined by

$$\varepsilon_i(k) = \frac{1}{L} \sum_{l=1}^L \left| \hat{\mathbf{x}}_{(i),k}^{(l)} - \mathbf{x}_{(i),k}^{(l)} \right| \quad (39)$$

where  $L$  is the number of Monte Carlo runs. Note that the performance evaluation indicators in the sequel include the averaged absolute error and the root mean square error, following the works [8, 16, 18]. Figure 2 plots the averaged



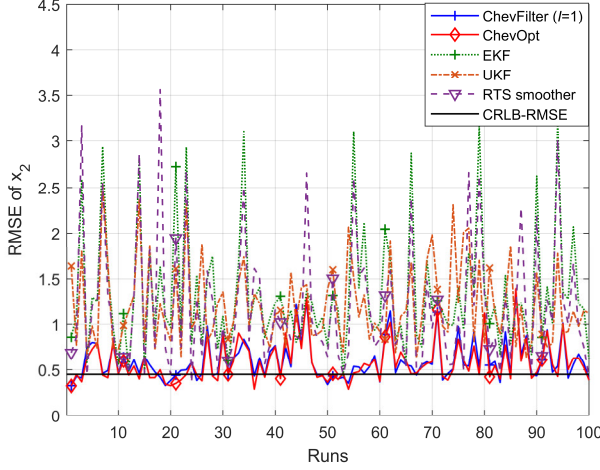


Fig. 4. RMSE of  $x_2$  (ChevFilter with window size of 1s) across 100 random runs and CRLB-RMSE.

TABLE I. ACCUMULATIVE RMSE IN EXAMPLE #1

	ChevFilter	ChevOpt	EKF	UKF	RTS Smoother	CRLB-RMSE
$x_1$	0.23	0.22	0.66	0.64	0.49	0.16
$x_2$	0.64	0.63	1.48	1.30	1.39	0.45

TABLE II. COMPARISON OF COMPUTATION COST IN EXAMPLE #1

	ChevFilter	ChevOpt	EKF	UKF	RTS Smoother
Time Cost (s)	0.07	0.81	0.02	0.10	0.16

absolute state errors of 100 Monte Carlo runs by different estimation algorithms and the square root of CRLB. We see that the ChevFilter and ChevOpt have the best accuracy, with the former being slightly worse than the latter. The list of the estimation accuracy in the ascending order is

$$\text{CRLB} > \text{ChevOpt} > \text{ChevFilter} > \begin{cases} \text{UKF} \\ \text{RTS smoother} \end{cases} > \text{EKF} \quad (40)$$

As we indicated in the introduction that EKF/RTS smoother and UKF make approximations about the dynamics and measurement nonlinearities by the first-order Taylor expansion and the deterministic sampling, respectively. In contrast, the proposed ChevOpt is an optimal state estimator in the MAP sense and the ChevFilter only makes a Gaussian assumption of the priori distribution. As a result, they achieve remarkably improved accuracy over EKF/RTS smoother and UKF.

The performance of different algorithms is also compared in terms of the root mean square error (RMSE), which is defined for  $l$ -th Monte Carlo run by

$$\text{RMSE}(l) = \sqrt{\frac{1}{K} \sum_{k=1}^K (\hat{\mathbf{x}}_k^{(l)} - \mathbf{x}_k^{(l)})^2} \quad (41)$$

where  $K$  is the number of time instants. And, the CRLB RMSE is defined by the root of averaging CRLB across  $K$  time instants, i.e.,

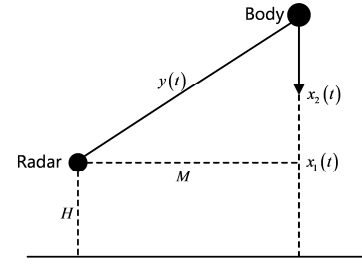


Fig. 5. Geometry of the ballistic target re-entry [14]

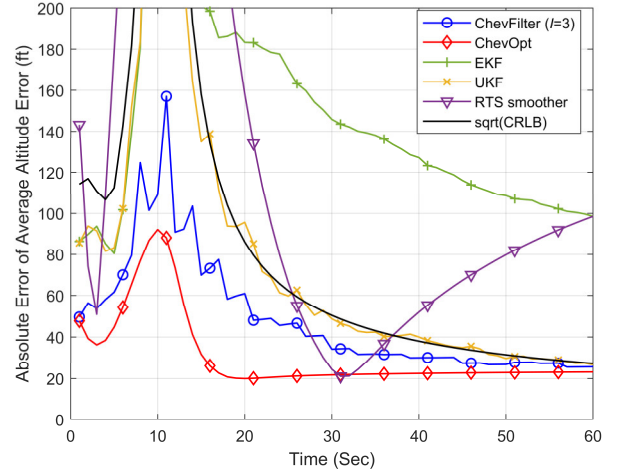


Fig. 6. Averaged absolute position errors (ChevFilter with window size 3s) and the square root of CRLB.

$$\text{CRLB-RMSE} = \sqrt{\frac{1}{K} \sum_{k=1}^K \text{CRLB}(k)} \quad (42)$$

Figures 3-4 plot the RMSE of the estimated state and CRLB across 100 Monte Carlo runs. The accumulative RMSE for each estimator is listed in Table I, which is calculated by

$$\text{ARMSE} = \sqrt{\frac{1}{LK} \sum_{l=1}^L \sum_{k=1}^K (\hat{\mathbf{x}}_k^{(l)} - \mathbf{x}_k^{(l)})^2} \quad (43)$$

These results clearly show the accuracy superiority of the ChevOpt and ChevFilter over the EKF/UKF and RTS smoother.

The average time cost of 100 Monte Carlo runs is listed in Table II. The time cost of ChevFilter is about 3 times larger than that of the EKF, yet still more efficient than UKF. Although the ChevOpt is about 40 times slower than EKF, it is intended for post-processing in lieu of real-time applications.

### B. Example 2: Ballistic Target Re-entry

This example is to estimate the altitude, velocity and ballistic coefficient of a vertically falling body as it re-enters the atmosphere at a very high altitude with high speed [59]. The geometry of this problem is shown in Fig. 5, where  $x_1(t)$  denotes the altitude,  $x_2(t)$  denotes the falling velocity, and  $y(t)$  is the measured distance between the radar and the body.

The altitude of the radar is  $H = 10^5$  feet and the horizontal distance between radar and the body is  $M = 10^5$  feet.

The continuous dynamic model is given as

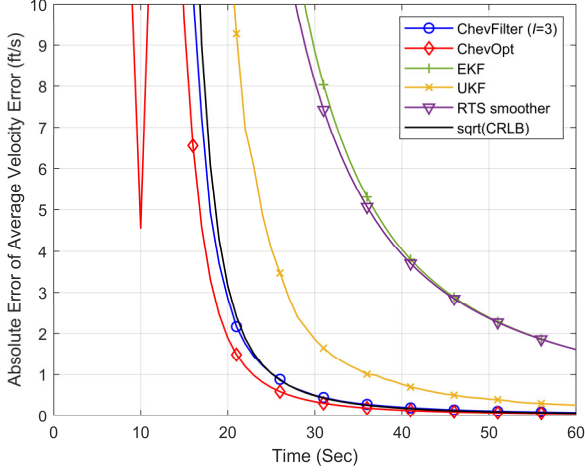


Fig. 7. Averaged absolute velocity errors (ChevFilter with window size 3s) and the square root of CRLB.

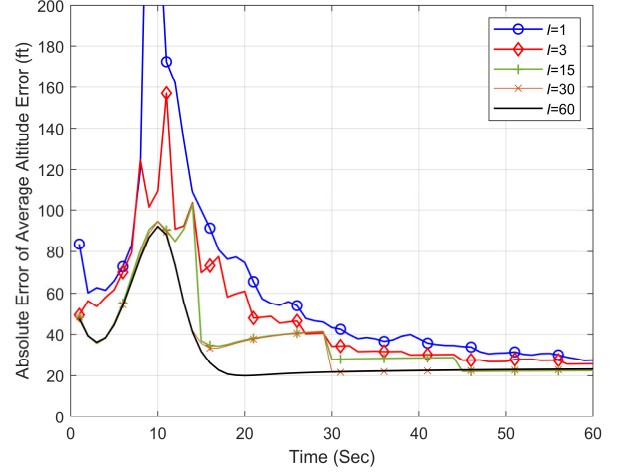


Fig. 9. Averaged absolute position errors of ChevFilter with different window sizes (1s, 3s, 15s, 30s and 60s).

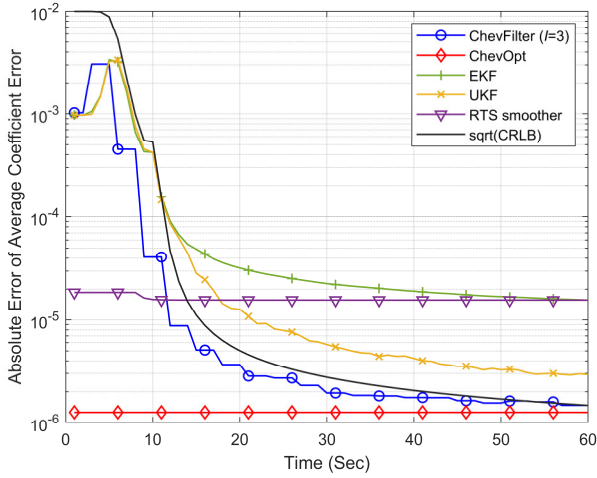


Fig. 8. Averaged absolute ballistic coefficient errors (ChevFilter with window size 3s) and the square root of CRLB.

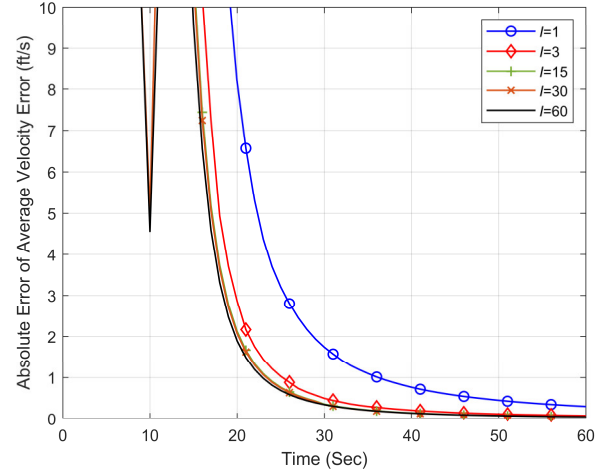


Fig. 10. Averaged absolute velocity errors of ChevFilter with different window sizes (1s, 3s, 15s, 30s and 60s).

$$\begin{aligned}\dot{x}_1(t) &= -x_2(t) + w_1(t) \\ \dot{x}_2(t) &= -e^{-\gamma x_1(t)} x_2^2(t) x_3(t) + w_2(t) \\ \dot{x}_3(t) &= w_3(t)\end{aligned}\quad (44)$$

where  $[w_1(t) \ w_2(t) \ w_3(t)]^T \sim N(\mathbf{0}, \mathbf{Q})$  and  $\gamma$  is a constant value ( $\gamma = 5 \times 10^{-5}$ ) that relates the air density with altitude. The radar measurement at time  $t_k$  is given as

$$y_k = \sqrt{(x_1(t_k) - H)^2 + M^2} + v_k \quad (45)$$

where  $v_k \sim N(0, R_k)$  and the measurement frequency is 1 Hz.

Following the previous literature [8, 14], the dynamic model has no noise, i.e.,  $\mathbf{Q} = 0$ , and the covariance of measurement noise is set to  $R_k = 10^4$ . The true initial state is  $\mathbf{x}_0 = [3 \times 10^5, 2 \times 10^4, 10^{-3}]^T$  and the initial state in the estimation is  $\hat{\mathbf{x}}_0 = [3 \times 10^5, 2 \times 10^4, 3 \times 10^{-5}]^T$  with the covariance given as

$$P_0 = \begin{bmatrix} 10^6 & 0 & 0 \\ 0 & 4 \times 10^6 & 0 \\ 0 & 0 & 10^{-4} \end{bmatrix}$$

To address the issue of semi-positive definiteness, the altitude  $x_1$  is represented using the velocity  $x_2$ 's Chebyshev coefficients as in Example 1 and the ballistic coefficient  $x_3$  is taken as a constant. As for the second dynamics equation in (44), we add a small disturbance  $w_2 \sim N(0, 0.001^2)$  to make it positive definite. Therefore, the estimation parameters of ChevFilter and ChevOpt in this example are defined as  $\mathbf{d} \triangleq [x_3 \ p_0 \ c_{0:N}^T]^T$ , where  $p_0$  and  $c_{0:N}^T$  are defined in (38).

To overcome the high nonlinearity of the dynamic model in (44), the differential equations are integrated by a fourth-order Runge-Kutta scheme with a step size of 1/64 seconds for both EKF and UKF. For this noise-free dynamic model, the CRLB is identical to the covariance matrix propagation of the EKF where the Jacobians are evaluated at the true state [8].



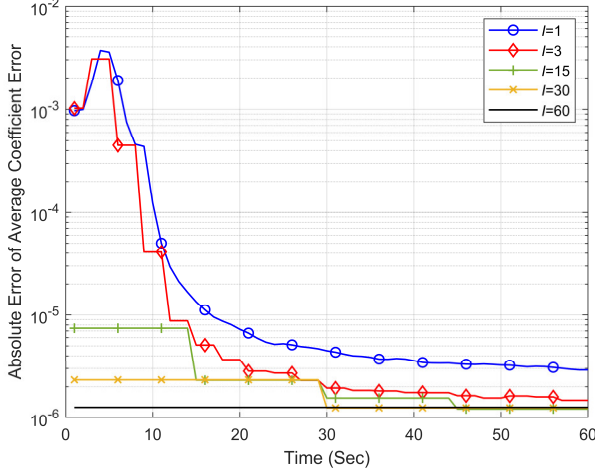


Fig. 11. Averaged absolute ballistic coefficient errors of ChevFilter with different window sizes (1s, 3s, 15s, 30s and 60s).

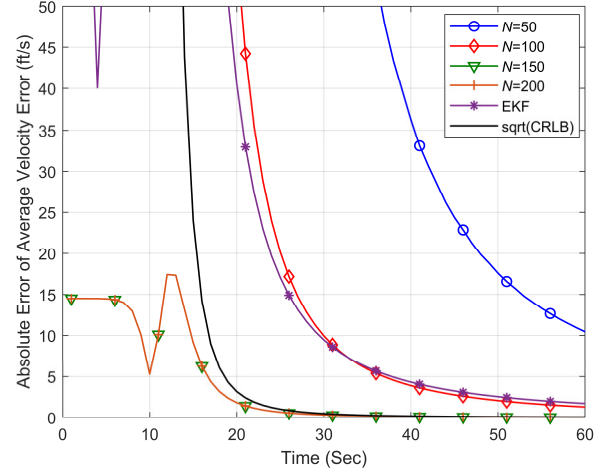


Fig. 13. Averaged absolute velocity errors of ChevOpt with different Chebyshev orders ( $N=50, 100, 150, 200$ ), EKF and the square root of CRLB.

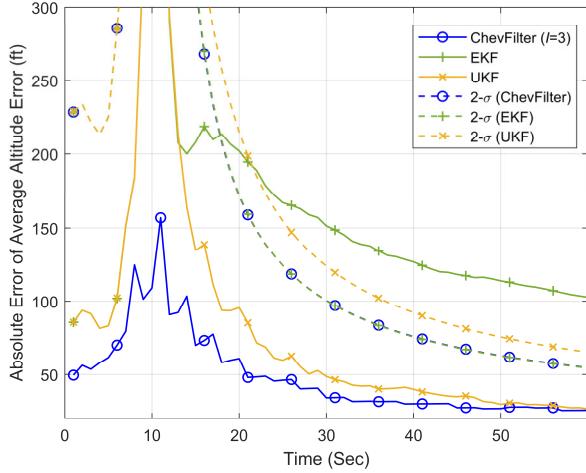


Fig. 12. Averaged absolute position errors with the associated 2-standard deviation bound (solid line for the estimate error and dotted line for the 2-standard deviation bound)

The averaged absolute errors of position, velocity and the ballistic coefficient by different estimators across 100 Monte Carlo runs are plotted in Figs. 6-8. The sliding window size of ChevFilter is 3 seconds. The Chebyshev polynomial orders of ChevFilter and ChevOpt are set to 20 and 150, respectively. The list of state estimation accuracy is

$$\text{ChevOpt} > \text{ChevFilter} > \text{CRLB} > \begin{cases} \text{UKF} \\ \text{RTS smoother} \end{cases} > \text{EKF} \quad (46)$$

It is surprising that the ChevFilter and ChevOpt achieve even better accuracy than the CRLB does in this example. This is arguably because the Chebyshev polynomial-based methods utilize all the measurements for each state estimate in the sliding window, in contrast to the CRLB using just up to and including the current measurement. Another reason may be that the nonlinearities of dynamics and measurement are better handled by the Chebyshev polynomial-based methods, as compared with the linearization model in the CRLB. For a sliding window of smaller size, however, the ChevFilter might be inferior to the CRLB, as shown below in Figs. 9-11.

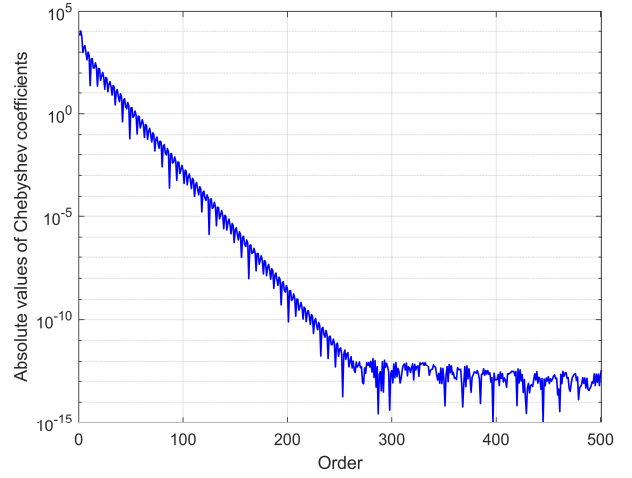


Fig. 14. Absolute values of Chebyshev coefficients of ChevOpt with Chebyshev polynomial order 500.

The position estimate errors and the associated  $2\sigma$  bounds are plotted in Fig. 12. The  $2\sigma$  bounds are computed as twice the averaged square root of diagonal elements of the covariance matrix. For a consistent filter, the estimation error should stay below the  $2\sigma$  derivation bounds with a possibility of 95%. Obviously, the ChevFilter and UKF are consistent, while the EKF are too optimistic with the estimation.

To evaluate the influence of the sliding window size, the averaged absolute state errors by ChevFilter with different window sizes ( $I = 1, 3, 15, 30$  and  $60$  seconds) are shown in Figs. 9-11. The corresponding Chebyshev polynomial orders are set to 10, 20, 80, 100 and 150, respectively. It is shown that the estimation accuracy improves along with the increasing size of the sliding window. Note that the ChevFilter with window size of 60 seconds is identical to the ChevOpt. With the increased window size, the effect of prior approximation in the optimization decreases and the ChevFilter approaches the ChevOpt. However, a larger window size brings about a longer time delay in carrying out the state estimation, as the estimation cannot be done until all the measurements in the sliding window come in. Therefore, the selection of the window size for

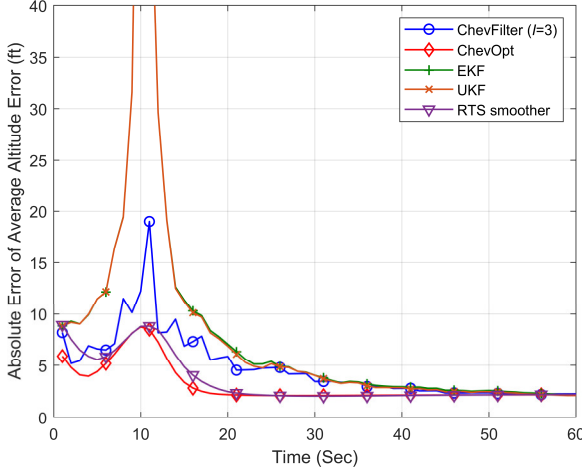


Fig. 15. Averaged absolute position errors with reduced measurement covariance (ChevFilter with window size 3s).

ChevFilter in real applications needs to consider the balance between the accuracy and the real-time requirement.

Another adjustable parameter that influences the accuracy of the estimation is the Chebyshev polynomial order to represent the state. A principle to set the Chebyshev polynomial order is to ensure that the Chebyshev polynomial approximation error is small enough in the state estimation. In the current implementation, the order of the Chebyshev polynomial requires to be manually prescribed, according to the dynamics of the model and the sliding window size. In general, high dynamics and large sliding window require a high-order Chebyshev polynomial to reduce the approximation error. But when the polynomial order is big enough, further increasing the order leads to heavy computer burden with little accuracy improvement. Figure 13 plots the averaged absolute velocity errors for the batch ChevOpt of different polynomial orders, in which the best performance is achieved when the Chebyshev polynomial order exceeds 150. A useful strategy to identify an appropriate polynomial order is by the convergence tendency and the absolute value of the estimated Chebyshev coefficients. Figure 14 plots the estimated Chebyshev coefficients of ChevOpt with polynomial order 500. We see that the Chebyshev coefficients converge exponentially before they reach the truncation error level at the order of about 270.

To examine the influence of the measurement noise, the measurement covariance in this simulation is reduced to  $R_k = 10^2$ . The averaged absolute position errors of 100 Monte Carlo runs are plotted in Fig. 15. Comparing with Fig. 6, the position estimation accuracy of all algorithms improves when the measurement covariance decreases. It can be seen that the proposed algorithms are still more accurate than other estimators, except that the RTS smoother becomes better than the ChevFilter in this case. This is because that the smoother is a batch estimation, which utilizes all the available measurements in the whole-time interval while the ChevFilter only uses the measurements in a small sliding window.

The average time cost across 100 Monte Carlo runs is plotted in Fig. 16. The time costs of ChevFilter with different window

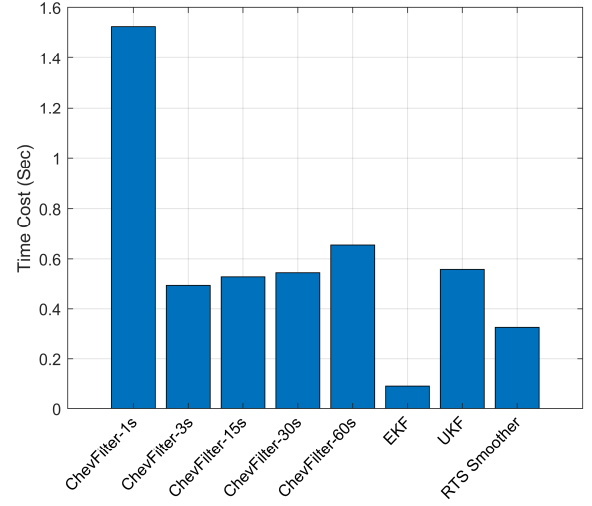


Fig. 16. Time costs of ChevFilter with different window sizes (1s, 3s, 15s, 30s and 60s), EKF, UKF and RTS smoother

sizes are comparable to that of UKF and about 5-6 times larger than that of EKF. An exception is for the window size of one second. The underlying reason is that a smaller window size leads to a decreased order of the Chebyshev polynomial but an increased number of sliding windows within a given time interval. In this regard, the size of sliding window should be carefully chosen for a specific application.

## VI. DISCUSSIONS AND CONCLUSIONS

This paper proposes a new continuous-time MAP estimation framework, in both batch and sliding window forms. Specifically, the continuous state over the time interval of interest is approximated by the Chebyshev polynomial and then the continuous MAP state estimation is transformed into a problem of Chebyshev coefficient optimization by the way of the Chebyshev collocation method. The proposed batch form, ChevOpt, is an optimal continuous-time estimation in the least squares sense; the sliding window form, ChevFilter, is suboptimal with the Gaussian approximation of the prior distribution. Numerical results of representative examples show that the proposed method results in much improved accuracy over the EKF, UKF and RTS smoother. A future work will explore more accurate prior approximation, e.g., representing the prior distribution by a Gaussian sum.

## APPENDIX [43]

This appendix provides the strategy to handle the non-positiveness of  $\mathbf{G}\mathbf{Q}\mathbf{G}^T$  in (5). Without the loss of generality,  $\mathbf{G}(t)\mathbf{w}(t)$  in (1) can be transformed to

$$\mathbf{G}(t)\mathbf{w}(t) = \bar{\mathbf{G}}(t)\bar{\mathbf{w}}(t) = \begin{bmatrix} \bar{\mathbf{G}}^{(1)}(t) \\ \bar{\mathbf{G}}^{(2)}(t) \end{bmatrix} \bar{\mathbf{w}}(t) \quad (47)$$

where  $\bar{\mathbf{G}}_1(t) \in \mathbb{R}^{r \times r}$  is a nonsingular matrix and  $\bar{\mathbf{w}} \in \mathbb{R}^r$  is the Gaussian noise with a positive definite covariance matrix  $\bar{\mathbf{Q}}(t)$ .

Then the dynamics in (1) is rewritten as

$$\dot{\mathbf{x}}(t) = \mathbf{f}(\mathbf{x}(t), \mathbf{u}(t)) + \bar{\mathbf{G}}(t)\bar{\mathbf{w}}(t) \quad (48)$$

Partitioning (48) into two sub-dynamics with  $r$  and  $n-r$  rows, it yields

$$\begin{bmatrix} \dot{\mathbf{x}}^{(1)}(t) \\ \dot{\mathbf{x}}^{(2)}(t) \end{bmatrix} = \begin{bmatrix} \mathbf{f}^{(1)}(\mathbf{x}(t), \mathbf{u}(t)) \\ \mathbf{f}^{(2)}(\mathbf{x}(t), \mathbf{u}(t)) \end{bmatrix} + \begin{bmatrix} \bar{\mathbf{G}}^{(1)}(t) \\ \bar{\mathbf{G}}^{(2)}(t) \end{bmatrix} \bar{\mathbf{w}}(t) \quad (49)$$

Define a nonsingular matrix  $\mathbf{L}(t)$  as

$$\mathbf{L}(t) = \begin{bmatrix} \mathbf{I}_r & \mathbf{0}_{r \times (n-r)} \\ -\bar{\mathbf{G}}^{(2)}(t)(\bar{\mathbf{G}}^{(1)}(t))^{-1} & \mathbf{I}_{n-r} \end{bmatrix} \quad (50)$$

where  $\mathbf{0}_{r \times (n-r)}$  denotes a  $r \times (n-r)$  zero matrix, and  $\mathbf{I}_r$  and  $\mathbf{I}_{n-r}$  denote identity matrices of  $r$  and  $n-r$  dimensions, respectively. Multiplying  $\mathbf{L}$  on both sides of (49) yields

$$\dot{\mathbf{y}}(t) = \begin{bmatrix} \dot{\mathbf{y}}^{(1)}(t) \\ \dot{\mathbf{y}}^{(2)}(t) \end{bmatrix} = \begin{bmatrix} \mathbf{g}^{(1)}(\mathbf{y}(t), \mathbf{u}(t)) \\ \mathbf{g}^{(2)}(\mathbf{y}(t), \mathbf{u}(t)) \end{bmatrix} + \begin{bmatrix} \bar{\mathbf{G}}^{(1)}(t) \bar{\mathbf{w}}(t) \\ \mathbf{0}_{(n-r) \times 1} \end{bmatrix} \quad (51)$$

where  $\dot{\mathbf{y}}(t) \triangleq \mathbf{L}(t)\dot{\mathbf{x}}(t)$  and the dynamics function  $\mathbf{g}(\mathbf{y}(t), \mathbf{u}(t)) \stackrel{y \leftarrow x}{=} \mathbf{L}(t)\mathbf{f}(\mathbf{x}(t), \mathbf{u}(t))$ . With the dynamics reformulated in (51), the original state estimation is transformed into that of the new state  $\mathbf{y}(t)$ , which consists of a sub-dynamics with positive definite noise matrix and a noise-free sub-dynamics.

## REFERENCES

- [1] F. L. Markley, and J. L. Crassidis, *Fundamentals of Spacecraft Attitude Determination and Control*: Springer, 2014.
- [2] M. Zhu, W. Ouyang, and Y. Wu, "Orientation estimation by partial-state updating Kalman filter and vectorial magnetic interference detection," *IEEE Transactions on Aerospace and Electronic Systems*, vol. 57, no. 3, pp. 1815-1826, 2021.
- [3] T. D. Barfoot, *State Estimation for Robotics*: Cambridge University Press, 2017.
- [4] A. I. Mourikis, and S. I. Roumeliotis, "A multi-state constraint Kalman filter for vision-aided inertial navigation," in *Proceedings of the 2007 IEEE International Conference on Robotics and Automation (ICRA)*, Rome, Italy, 2007, pp. 3565-3572.
- [5] J. D. Murray, *Mathematical Biology*, New York: Springer, 1993.
- [6] Y. C. Ho, and R. C. K. Lee, "A Bayesian approach to problems in stochastic estimation and control," *IEEE Transactions on Automatic Control*, vol. 9, no. 4, pp. 333-339, 1964.
- [7] R. E. Kalman, "A new approach to linear filtering and prediction problems," *Journal of Basic Engineering*, vol. 82, pp. 34-45, 1960.
- [8] Y. Wu, D. Hu, M. Wu, and X. Hu, "A numerical-integration perspective on Gaussian filters," *IEEE Transactions on Signal Processing*, vol. 54, no. 8, pp. 2910-2921, 2006.
- [9] K. Ito, and K. Q. Xiong, "Gaussian filters for nonlinear filtering problems," *IEEE Transactions on Automatic Control*, vol. 45, no. 5, pp. 910-927, 2000.
- [10] S. Sarkka, and J. Sarmavuori, "Gaussian filtering and smoothing for continuous-discrete dynamic systems," *Signal Processing*, vol. 93, no. 2, pp. 500-510, 2013.
- [11] B. Ristic, S. Arulampalam, and N. Gordon, *Beyond the Kalman Filter: Particle Filters for Tracking Applications*: Artech house, 2003.
- [12] S. F. Schmidt, "The Kalman filter-Its recognition and development for aerospace applications," *Journal of Guidance Control and Dynamics*, vol. 4, no. 1, pp. 4-7, 1981.
- [13] A. Gelb, *Applied Optimal Estimation*, Cambridge, MA: MIT Press, 1974.
- [14] J. L. Crassidis, and J. L. Junkins, *Optimal Estimation of Dynamic Systems*: Chapman and Hall/CRC, 2011.
- [15] S. Julier, J. Uhlmann, and H. F. Durrant-Whyte, "A new method for the nonlinear transformation of means and covariances in filters and estimators," *IEEE Transactions on Automatic Control*, vol. 45, no. 3, pp. 477-482, 2000.
- [16] S. Sarkka, "On unscented kalman filtering for state estimation of continuous-time nonlinear systems," *IEEE Transactions on Automatic Control*, vol. 52, no. 9, pp. 1631-1641, 2007.
- [17] I. Arasaratnam, S. Haykin, and R. J. Elliott, "Discrete-time nonlinear filtering algorithms using Gauss-Hermite quadrature," *Proceedings of the IEEE*, vol. 95, no. 5, pp. 953-977, 2007.
- [18] I. Arasaratnam, S. Haykin, and T. R. Hurd, "Cubature Kalman filtering for continuous-discrete systems: theory and simulations," *IEEE Transactions on Signal Processing*, vol. 58, no. 10, pp. 4977-4993, 2010.
- [19] I. Arasaratnam, and S. Haykin, "Cubature Kalman filters," *IEEE Transactions on Automatic Control*, vol. 54, no. 6, pp. 1254-1269, 2009.
- [20] J. H. Kotecha, and P. M. Djuric, "Gaussian sum particle filtering," *IEEE Transactions on Signal Processing*, vol. 51, no. 10, pp. 2602-2612, 2003.
- [21] O. Cappe, S. J. Godsill, and E. Moulines, "An overview of existing methods and recent advances in sequential Monte Carlo," *Proceedings of the IEEE*, vol. 95, no. 5, pp. 899-924, 2007.
- [22] A. Doucet, and A. M. Johansen, *A Tutorial on Particle Filtering and Smoothing: Fifteen Years Later*, Oxford, U.K.: Oxford Univ. Press, 2009.
- [23] M. Kaess, H. Johannsson, R. Roberts, V. Ila, J. J. Leonard, and F. Dellaert, "iSAM2: Incremental smoothing and mapping using the Bayes tree," *The International Journal of Robotics Research*, vol. 31, no. 2, pp. 216-235, 2012.
- [24] F. Dellaert, and M. Kaess, "Factor graphs for robot perception," *Foundations and Trends in Robotics*, vol. 6, no. 1-2, pp. 1-139, 2017.
- [25] D. G. Robertson, J. H. Lee, and J. B. Rawlings, "A moving horizon-based approach for least-squares estimation," *AIChE Journal*, vol. 42, no. 8, pp. 2209-2224, 1996.
- [26] C. V. Rao, J. B. Rawlings, and D. Q. Mayne, "Constrained state estimation for nonlinear discrete-time systems: stability and moving horizon approximations," *IEEE Transactions on Automatic Control*, vol. 48, no. 2, pp. 246-258, 2003.
- [27] A. Alessandri, M. Baglietto, and G. Battistelli, "Moving-horizon state estimation for nonlinear discrete-time systems: new stability results and approximation schemes," *Automatica*, vol. 44, no. 7, pp. 1753-1765, 2008.
- [28] P. Furgale, T. D. Barfoot, and G. Sibley, "Continuous-time batch estimation using temporal basis functions," in *IEEE International Conference on Robotics and Automation (ICRA)*, 2012, pp. 2088-2095.
- [29] P. Furgale, J. Rehder, and R. Siegwart, "Unified temporal and spatial calibration for multi-sensor systems," in *IEEE/RSJ International Conference on Intelligent Robots and Systems*, 2013, pp. 1280-1286.
- [30] P. Furgale, C. H. Tong, T. D. Barfoot, and G. Sibley, "Continuous-time batch trajectory estimation using temporal basis functions," *International Journal of Robotics Research*, vol. 34, no. 14, pp. 1688-1710, 2015.
- [31] H. Ovrén, and P. E. Forssén, "Trajectory representation and landmark projection for continuous-time structure from motion," *The International Journal of Robotics Research*, vol. 38, no. 6, pp. 686-701, 2019.
- [32] H. Ovrén, and P. E. Forssén, "Spline error weighting for robust visual-inertial fusion," in *IEEE Conference on Computer Vision and Pattern Recognition*, Salt Lake City, 2018, pp. 321-329.
- [33] J. P. Boyd, *Chebyshev and Fourier Spectral Methods*, 2 ed.: Courier Corporation, 2001.
- [34] L. N. Trefethen, *Approximation Theory and Approximation Practice*: SIAM, 2019.
- [35] C. Canuto, M. Y. Hussaini, A. Quarteroni, and T. A. Zang, *Spectral Methods in Fluid Dynamics*, New York: Springer-Verlag, 1988.
- [36] B. Fornberg, *A Practical Guide to Pseudospectral Methods*, New York: Cambridge university press, 1998.
- [37] D. Garg, M. Patterson, W. W. Hager, A. V. Rao, D. A. Benson, and G. T. Huntington, "A unified framework for the numerical solution of optimal control problems using pseudospectral methods," *Automatica*, vol. 46, no. 11, pp. 1843-1851, 2010.
- [38] M. Kelly, "An introduction to trajectory optimization: How to do your own direct collocation," *SIAM Review*, vol. 59, no. 4, pp. 849-904, 2017.
- [39] F. Fahroo, and I. M. Ross, "Direct trajectory optimization by a chebyshev pseudospectral method," *Journal of Guidance, Control, and Dynamics*, vol. 25, no. 1, pp. 160-166, 2002.
- [40] Q. Chen, Y. Zhang, S. Liao, and F. Wan, "Newton-Kantorovich/pseudospectral solution to perturbed astrodynamics two-point boundary-value problems," *Journal of Guidance, Control, and Dynamics*, vol. 36, no. 2, pp. 485-498, 2013.
- [41] T. A. Elgohary, J. L. Junkins, and S. N. Atluri, "An RBF-collocation algorithm for orbit propagation," in *Advances in Astronautical Sciences: AAS/AIAA Space Flight Mechanics Meeting*, Williamsburg, USA, 2015.

- [42] V. Agrawal, and F. Dellaert, "Continuous-time state & dynamics estimation using a pseudo-spectral parameterization," in *IEEE International Conference on Robotics and Automation (ICRA)*, China, 2021, pp. 426-432.
- [43] A. H. Jazwinski, *Stochastic Process and Filtering Theory*, NY, USA: Academic Press, 1970.
- [44] Y. Wu, "RodFilter: attitude reconstruction from inertial measurement by functional iteration," *IEEE Transactions on Aerospace and Electronic Systems*, vol. 54, no. 5, pp. 2131-2142, 2018.
- [45] Y. Wu, Q. Cai, and T.-K. Truong, "Fast RodFilter for attitude reconstruction from inertial measurement," *IEEE Transactions on Aerospace and Electronic Systems*, vol. 55, no. 1, pp. 419-428, 2019.
- [46] Y. Wu, and G. Yan, "Attitude reconstruction from inertial measurements: QuatFilter and its comparison with RodFilter," *IEEE Transactions on Aerospace and Electronic Systems*, vol. 55, no. 6, pp. 3629-3639, 2019.
- [47] Y. Wu, "iNavFilter: next-generation inertial navigation computation based on functional iteration," *IEEE Transactions on Aerospace and Electronic Systems*, vol. 56, no. 3, pp. 2061-2082, 2020.
- [48] P. Cheng, M. Chen, V. Stojanovic, and S. He, "Asynchronous fault detection filtering for piecewise homogenous Markov jump linear systems via a dual hidden Markov model," *Mechanical Systems and Signal Processing*, vol. 151, pp. 107353, 2021.
- [49] Fang H, S. V. Zhu G, and e. al., "Adaptive optimization algorithm for nonlinear Markov jump systems with partial unknown dynamics," *International Journal of Robust and Nonlinear Control*, vol. 31, no. 6, pp. 2126-2140, 2021.
- [50] W. H. Press, S. A. Teukolsky, W. T. Vetterling, and B. P. Flannery, *Numerical Recipes : the Art of Scientific Computing*, 3 ed.: Cambridge University Press, 2007.
- [51] J. Shen, and T. Tang, *Spectral and High-Order Methods with Applications*, China: Science Press, 2006.
- [52] S. Olver, and A. Townsend, "A fast and well-conditioned spectral method," *SIAM Review*, vol. 55, no. 3, pp. 462-489, 2013.
- [53] J. Nocedal, and S. Wright, *Numerical Optimization*: Springer Science & Business Media, 2006.
- [54] L. N. Trefethen, "Is Gauss quadrature better than Clenshaw-Curtis?," *SIAM Review*, vol. 50, no. 1, pp. 67-87, 2008.
- [55] S. J. Julier, and J. K. Uhlmann, "'Corrections to "unscented filtering and nonlinear estimation," *Proceedings of the IEEE*, vol. 92, no. 12, pp. 1958-1958, 2004.
- [56] G. Y. Kulikov, and M. V. Kulikova, "Accurate numerical implementation of the continuous-discrete extended Kalman filter," *IEEE Transactions on Automatic Control*, vol. 59, no. 1, pp. 273-279, 2014.
- [57] P. Tichavsky, C. H. Muravchik, and A. Nehorai, "Posterior Cramér-Rao bounds for discrete-time nonlinear filtering," *IEEE Transactions on Signal Processing*, vol. 46, no. 5, pp. 1386-1396, 1998.
- [58] P. E. Kloeden, and E. Platen, *Numerical Solution of Stochastic Differential Equations*: Springer Science & Business Media, 2013.
- [59] M. Athans, R. Wishner, and A. Bertolini, "Suboptimal state estimation for continuous-time nonlinear systems from discrete noisy measurements," *IEEE Transactions on Automatic Control*, vol. 13, no. 5, pp. 504-514, 1968.